Chemistry induced during the thermalization and transport of positrons and secondary electrons in gases and liquids



2015 Plasma Sources Sci. Technol. 24 025016

(http://iopscience.iop.org/0963-0252/24/2/025016)

IOP Publishing Plasma Sources Science and Technology

Plasma Sources Sci. Technol. **24** (2015) 025016 (7pp) doi:10.1088/0963-0252/24/2/025016

# Chemistry induced during the thermalization and transport of positrons and secondary electrons in gases and liquids

**S Marjanović[1], A Banković[1], R D White[2], S J Buckman[3,5], G Garcia[4], G Malović[1], S Dujko[1] and Z Lj Petrović[1,6]**

[1] Institute of Physics, University of Belgrade, Pregrevica 118, 11080 Belgrade, Serbia
[2] ARC Centre for Antimatter–Matter Studies, School of Engineering and Physical Sciences, James Cook University, Townsville 4810, QLD, Australia
[3] ARC Centre for Antimatter–Matter Studies, Research School of Physics and Engineering, Australian National University, Canberra, ACT 0200, Australia
[4] Instituto de Física Fundamental, Consejo Superior de Investigaciones Cientıficas, 28006 Madrid, Spain
[5] Institute of Mathematical Sciences, University of Malaya, Kuala Lumpur, Malaysia
[6] Serbian Academy of Sciences and Arts, Belgrade 11000, Serbia

E-mail: zoran@ipb.ac.rs (Z Lj Petrović)

Received 14 October 2014, revised 25 December 2014
Accepted for publication 21 January 2015
Published 2 March 2015


**Abstract**

The recent availability of cross sections for positron (and positronium) interactions has made it possible to calculate transport properties and rates of collisions, and study in a quantitative fashion some aspects of positron-induced processes and their effects on living tissue. This paper models the interaction of primary positrons, and their secondary electrons, with water vapour (and subsequently liquid) using complete sets of cross sections predominately based on experimental binary collision data. We use a simple procedure to represent the presence of organic molecules where we look for dissociation of methane as a prototype of organic molecule dissociation. We isolate this particular process in order to establish whether the degree of damage is directly associated with the energy deposited in the tissue or whether some specific processes may cause excessive damage even with little energy deposition. We thus report on the relative contributions of initial positrons and secondary electrons in inducing dissociation, the spatial and energy profiles of individual collisional events, and positron/secondary electron tracks. It was found that secondary electrons induce 2–3 times more dissociations than the original positrons and with a longer range.

Keywords: Monte Carlo simulation, radiation damage, dissociation, positrons, electrons

(Some figures may appear in colour only in the online journal)

## 1. Introduction

When considered independently, positrons in gases are seldom associated with induced chemistry. Some studies of positron-induced dissociation and resulting fragment molecules have been published [1, 2]. However, most of the reactions induced by positrons in living tissues may be regarded as chemical in nature and also as a potential source of dangerous radiation damage to live organisms. Thus chemical effects of positrons become very important for their biomedical applications.

Positron transport in gases is controlled by the same processes as for electrons—external fields and collisions with gas molecules. The essential difference is twofold: first there is no multiplication, so a plasma cannot be formed without

 

an external source of positrons, and second, the cross-section for positronium (Ps) formation as a loss process exceeds a similar loss process for electrons, that of attachment, by several orders of magnitude. On the other hand, positrons may induce the same plasma chemical processes as electrons. The effect may be through secondary electrons, or in direct collisions of positrons with molecules. Recently, a number of atomic and molecular collision cross sections for positrons have become available, thus making it possible to develop complete sets of cross sections (i.e. sets that include all important processes for a certain gas so that the number, energy and momentum balances are preserved) [3] and hence to model processes in gases by using kinetic schemes developed for low temperature non-equilibrium plasmas.

Using complete sets of cross sections for a number of gases, we have calculated transport coefficients such as drift velocities, diffusion coefficients, characteristic energies and rate coefficients for all collision processes, including number-changing process such as Ps formation [4–9]. The non-conservative nature of Ps formation induces effects in transport coefficients such as a very large difference between bulk and flux transport properties for the drift velocity and longitudinal diffusion [4–8]. For the bulk drift velocity, negative differential conductivity [8] is even induced when it is not present in the flux drift velocity. We have also calculated average properties such as the range of positrons and their secondary electrons, thermalization development in time, and finally the energy loss function [9]. We also calculate tracks of positrons, Ps and secondary electrons in water vapour. Recently a theory has been developed by White and colleagues which describes how to define cross sections for collisions in liquids, albeit for non-polar molecules [10–13]. In this paper we use kinetic approach to model positron and secondary electron transport in a rather simple model of the living tissue.

Newly measured cross-section data for positron interaction with organic matter include molecules like formic acid, uracil and $\alpha$-tetrahydrofurfuryl alcohol [14–17] and any of these molecules would represent a good addition to the model for the investigation of positron interactions with tissue. However there is still insufficient data to form a complete cross-section set, which is required for the simulation, so further work in that field is needed. That is why the water molecule, water being the main ingredient of living organisms, is still the basic model for the behaviour of positrons in human tissue [18]. Papers have been reported in the literature on calculations of positron cross sections for water vapour [19] and other molecules [20] using approximate theoretical methods. Those have represented a major improvement in radiation damage codes, as previously either no calculations have been made for positron-induced radiation damage, or calculations were based mostly on the data for electrons.

To date, the primary goal of studies of the effects of positrons on living tissue was to elucidate tracks of positrons in water vapour as an analogue for living tissue [21–23]. With a large body of new experimental data [14–17, 24], further simulations should be based primarily on accurately measured scattering data where possible, and some improved theoretical analyses.

Before we proceed we need to elaborate on three points. First, one has to be aware that our work is an extension of the usual treatment of positron effects in the living tissue that is a part of standard radiation damage packages such as PENELOPE [25] or GEANT-4 [26]. The basis for those codes is the assumption of the gas phase collisions, which is an improvement on the older techniques that were based on energy deposition measurements. However, as it has been postulated, some of the damage may arise from the atomic and molecular processes, and is most likely to be in poor correlation to the deposited energy. Most of these processes such as dissociative attachment [27] have very low energy losses and originate from the quasi-thermal region of the electron distribution.

Second is the issue of transport in liquids versus transport in gases. While some attempts have been made to transfer the phenomenology of the solid state transport to liquids [28] mostly the radiation therapy models are based on gas phase collisions. Building the liquid phenomenology from binary collisions onward is difficult, but some crucial steps have been made. White and co-workers have added structural factors to scattering to describe multiple scattering effects [10] and extended their work to water vapour [13]. Other theories exist with different phenomenologies and it is rather difficult to pinpoint whether all those effects are separate, or overlapping, or the same. We have to point out that electrons in water tend to be hydrated and the binding energy is of the order of 5 eV [29]. This value coincides with the conclusion of White *et al* that, above 5 eV, effects of multiple scattering are negligible due to a smaller de Broglie wavelength. Although we have some of the data for low energy dissociative attachment of DNA components [17, 30], and we have used them in calculations, we decided to stay clear of energies below 5 eV and to use data for dissociation of $CH_4$ by electrons as a representation of direct dissociation both by positron and secondary electron impact.

Finally we need to point out that it is a standard technique in swarm physics to assume that some molecules, present in a small abundance, may be represented by a single process, assuming that other properties of that molecule do not affect energy, momentum and other balances, and thus the energy distribution function of the mixture is the same as in the pure buffer gas. This technique has been often used in the determination of attachment coefficients in a number of gases even, without knowing the other cross sections for those gases [31]. In this case we assume that organic content does not modify the distribution function of either positrons or secondary electrons, and thus we represent the organic content by water in all respects, while adding one specific process (dissociation of $CH_4$) that is being analysed. Our model is a very simple representation of the human tissue. It however shows how initial steps in chemical reactions originate from the initial positrons, and their secondaries, within the assumption of using water as a model of the living tissue.

## 2. Monte Carlo simulation: procedure and the data

We employ a Monte Carlo simulation (MCS) based on a detailed, and hopefully complete, cross-section set. The simulation follows all collisions and randomly selects their

properties from the input data (total and differential cross sections, partition of energy upon ionization, etc) so, that on average, the probabilities of events follow the independently measured cross sections. Also we take care that conservation laws are satisfied (number, momentum and energy). The Monte Carlo procedure has been described in several of our papers [32–35]. As this code originated from a code for the simulation of electron swarms and standard gas discharges, the code has passed all the benchmark tests in both electric, and combinations of electric and magnetic fields. In that respect, the code is being used as a source of benchmarks [32, 34, 36]. In particular the code has the provision for the accurate determination of relative-velocity-based collision frequency that has been proposed and tested in [34]. This collision frequency is evaluated by solving the integral:

$$\nu(v) = \frac{n}{\sqrt{\pi} w v} \int_0^{+\infty} \mathrm{d}x \sigma(x) x^2 \times \left\{ \exp\left[ -\frac{(x-v)^2}{x^2} \right] - \exp\left[ -\frac{(x+v)^2}{x^2} \right] \right\}, \quad (1)$$

where $v$ is the particle velocity, $w$ is the most probable thermal velocity of the background gas and $\sigma$ is the cross-section for the process in question. Then the moment of collision is determined from the probability density

$$p(t) = \nu(t) \exp\left[ -\int_0^t \mathrm{d}t' \nu\left(t'\right) \right], \quad (2)$$

by solving the equation

$$\int_0^t \mathrm{d}t' \mathrm{p}\left(t'\right) = r, \quad (3)$$

where $r$ is a uniform random number from [0,1]. For more details the reader is referred to [32–35].

A particular feature of the MCS is that complete sets of cross sections are used thus ensuring the conservation of all relevant quantities. While this is easily tested for electrons, through modelling of swarm data, the required data for positrons are missing and the sets cannot be validated. While it is possible to set up positron swarm experiments [37–39], the data are still not available. In principle, calculations of individual trajectories, while producing visual representation of the events, cannot be used to test the codes as each trajectory is very much different from others. Thus we suggest using averaged properties such as: range, thermalization time, radial profiles of particle numbers and deposited energy and radial profiles of different events [9]. Such properties provide some test of the energy balance, number balance and even momentum balance. They are also more easily measured, and so some of the data is available.

In simulations, we follow all the positrons until they are annihilated (mostly through Ps formation) and also all the secondary electrons and their collisions. Thus, we add a very important range of effects due to electrons that may induce chemical dissociative processes against complex organic molecules such as DNA [30].

As for the input data, we use the cross sections for positrons in water vapour [3, 4, 9, 24] which have been tested and used to analyse the swarm properties in $H_2O$ [4]. It is still a water vapour model of the tissue but it has been shown by White *et al* [10, 13]. that in a liquid, multiple scattering generally affects only collisions below 5 eV, and that is mainly in the momentum transfer. Most important events in this simulation occur above 5 eV. In a similar fashion, a well-documented cross-section set for electrons in water vapour has been used for their trajectories [3].

In the living tissue, water is the dominant background molecule but there would be a large number of organic molecules as well. In our first step towards simulating positron-induced chemistry in living tissue, we shall assume that positrons develop their trajectories in the water vapour background. To represent processes leading to chemistry, we shall first include one process, dissociative excitation of $CH_4$, which is in actuality the breaking of a C–H bond (plus excitation) by a particle with sufficient energy. We have added a cross-section for this process [40, 41] to some molecules bearing otherwise the water cross sections, where we effectively assume that the additional 'organic' molecules do not affect the total energy, momentum and number balances, and we just project the events related to this process to the transport of positrons in pure $H_2O$. The same dissociative excitation cross-section is assumed for both positrons and electrons. In other words, we assume that 'organic' molecules have the same cross sections as the water vapour with only one additional process. The uncertainties in the cross-section for dissociative excitation will affect the rate of events but the general conclusion on the relative contribution of the two processes (by electrons and by positrons) will remain the same.

The idea is to compare pure water and 'organic' (mixture) data. We have added the C–H bond dissociation representation to 10% of the water vapour molecules. Basically we seek to check whether these processes would be sufficiently numerous, and how they are distributed in space arising from both the initial positrons and secondary electrons.

Energy partitioning in ionization events for both positrons and electrons is modelled after the standard approach for electrons [42]. The simulation was done with 50 000 initial positrons, all starting with 800 eV energy in the gas at atmospheric pressure. Starting energy of 800 eV provides enough collisions for positrons before they reach lower energies, which allows the simulated positron energy distribution to become a good representation of a thermalizing particle swarm. It is also an optimal choice with a good coverage of pertinent processes by accurately measured or calculated binary collision data.

## 3. Positron tracks in mixtures of water and organic material

In several publications, positron (and electron) tracks have been shown as a representation of the interaction of positrons with the background gas ( [9] and references therein). In particular, tracks in water vapour were followed [22, 23, 43]. Here we shall show the positron tracks augmented by the tracks of all secondary electrons. The positron trajectory is connected, starting at the positron emission point and ending with Ps formation (star and X respectively) in a similar

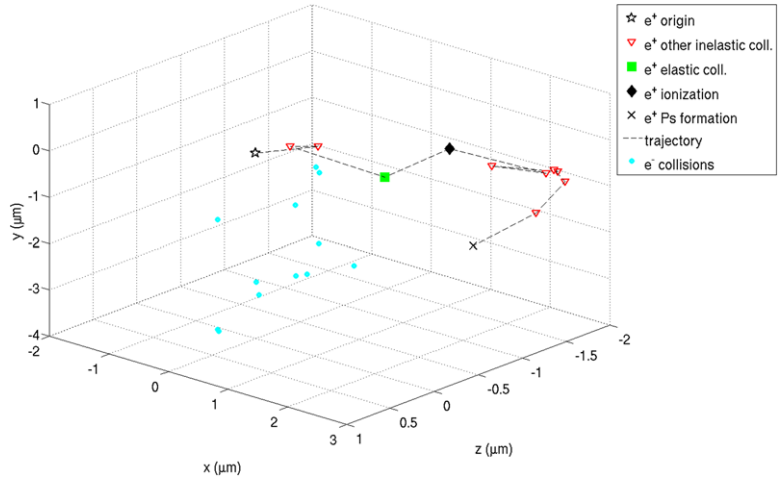


**Figure 1.** The trajectory of a positron emitted with 800 eV of energy which has undergone Ps formation after only several collisions. Only one secondary electron was generated on this track, and also there were no dissociations produced.

fashion as in [9]. After the Ps formation, the particle is not followed anymore, and any damage caused by gamma rays following positron annihilation is left to a separate analysis. In figure 1, we show an example of a positron track where only one secondary electron was formed. The collisions of secondary electrons are plotted as small dots (light blue) and are not connected for better visibility. The trajectory of the positron is connected by the dashed line. However, such trajectories, are very improbable. More frequently, a positron undergoes several ionizations before reaching energies where Ps formation is dominant.

In an extended trajectory with many more collisions (see figure 2), there are also numerous secondary electrons generated (around 10). In addition, we see several dissociations due to direct collisions with positrons. On the other hand we see that the range of electrons extends over a much larger volume and with a larger range. The collisions are numerous and, while dissipating smaller amounts of energy, they still may produce a significant amount of damage. This is observed in a number of electron-induced dissociations, marked as solid (blue) stars. The number of such dissociations exceeds the number of direct positron-induced processes. The range is also larger. However, these effects will vary from track to track, and may be quite different for some tracks, even if the initial conditions are the same. Thus we believe that overall averages are a better representation of the onset of the relevant chemical reactions.

## 4. Space/energy profiles and averages of collisions of positrons and secondary electrons

Here we take thousands of trajectories and average over them to obtain different observables in order to make comparisons and general conclusions. A quite common procedure in radiation therapy is to observe the energy that is deposited into the tissue. In figure 3, we show energies deposited per positron at different distances from the origin. Our technique enables us to separate all processes and their contributions as a function of the range. In other words, this figure represents the spatially resolved distribution of energy loss due to all collision events, at different distances from the origin of positrons, normalized to the number of initial positrons. In the case of non-conservative collisions (Ps formation), the entire energy of the projectile is sampled as the energy loss as it is removed from the particle swarm and delivered as a pair of gamma rays. This process gives a moderate contribution to the energy loss at small to moderate ranges up to 15 $\mu$m. In the same range, 10 times higher contributions are made by positron-induced ionization, electron-induced ionization and excitation. The dissociation as defined above, contributes approximately as much as Ps formation energy loss. At greater distances however, positrons do not contribute significantly as their ranges are much shorter than those of electrons. The spatial profiles for positrons and electrons differ, with positrons peaking closer to the origin and electrons having ranges almost two times greater. The dissociative processes induced by positrons follow the profile for positrons while those induced by electrons follow the energy deposition profile for secondary electrons. In total, kinetic energy deposited by electrons is several times larger than that deposited by positrons.

Figure 4 represents the spatial distribution of collision events, per unit length, normalized to the number of initial positrons. The position (distance from the origin/source) of each collision was sampled and associated with the appropriate collision-type distribution. We can see that positron-induced rotational collisions, due to a large number of rotational transitions, and electron-induced vibrational collisions are all associated with very small energy losses. The fractions of Ps formation and ionization collisions are relatively small compared to other processes but those define the growth of the number of charged particles and their branching in tracks. Again, electron-induced processes extend further away from the source, and are more abundant due to the fact that approximately ten electrons are produced per single positron.

Figure 5 represents the distribution of collision events according to the incident energy of the projectile (positron or electron) during thermalization of positrons and secondary electrons. The incident energy of the projectile is sampled

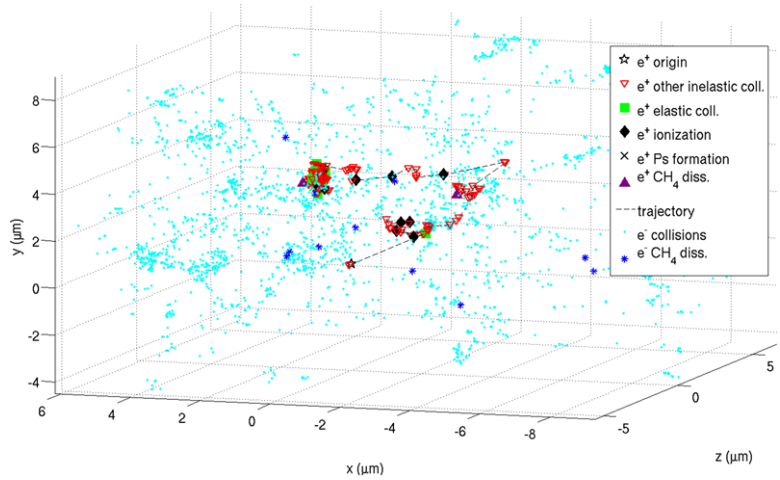


**Figure 2.** The trajectory of a positron emitted with 800 eV of energy in which a large number of secondary electrons are formed before the formation of Ps. Around 10 secondary electrons initiate their trajectories, illustrated here by a large number of points depicting collision events for electrons. The induced dissociative processes are highlighted as solid blue stars.

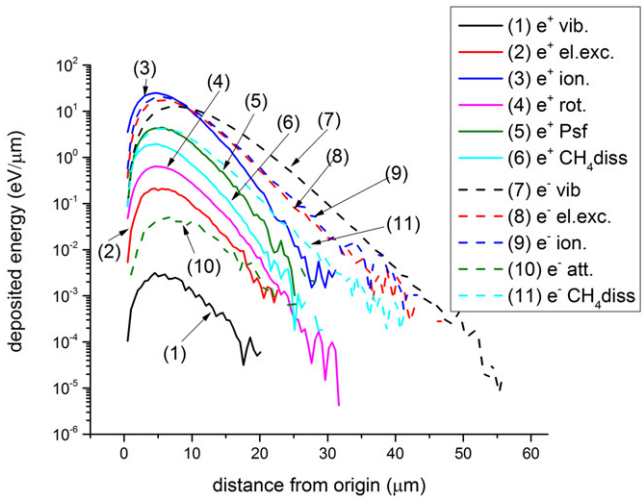


**Figure 3.** Spatial dependence of the energy deposited to the medium by positrons and secondary electrons per single positron, for different types of collisions. Solid lines represent positron collisions (1—vibrational excitation, 2—electron excitation, 3—ionization, 4—rotational excitation, 5—Ps formation, 6—$CH_4$ dissociation), while the dashed lines represent electron collisions (7—vibrational excitation, 8—electron excitation, 9—ionization, 10—attachment, 11—$CH_4$ dissociation).

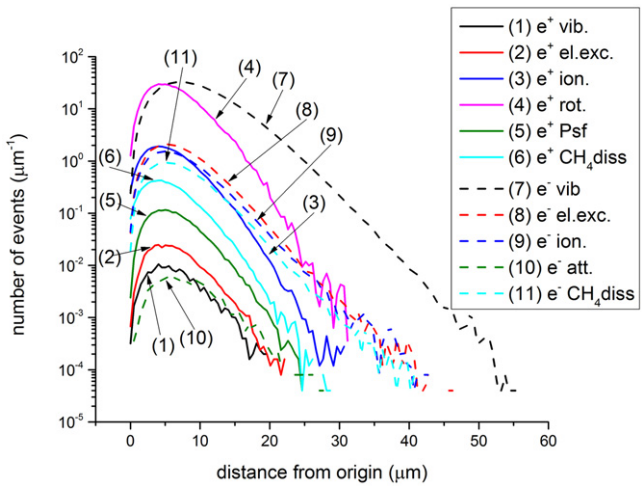


**Figure 4.** Distribution of collision events as a function of the distance from the origin. Solid lines represent positron collisions (1—vibrational excitation, 2—electron excitation, 3—ionization, 4—rotational excitation, 5—Ps formation, 6—$CH_4$ dissociation), while the dashed lines represent electron collisions (7—vibrational excitation, 8—electron excitation, 9—ionization, 10—attachment, 11—$CH_4$ dissociation).

and associated with the appropriate collision-type distribution, and normalized to the number of initial positrons. The peak at 800 eV in positron curves arises from the fact that the positrons all start from that initial energy. The subsequent dip in curves below that energy is a result of energy loss by positrons in ionization (predominantly) events where positrons lose enough energy to effectively skip, and undergo less collisions in this energy region. Further collisions lead to broadening of the positron energy distribution and therefore such structures are no longer observed. We note, that the electron-induced processes peak at low energies. This follows as the secondary electrons arising from ionization processes have energy distributions lower than the positron emission energy distributions.

## 5. Conclusion

We have summarized how the same techniques, used to describe the basic transport, trapping and plasma chemistry induced by electrons, may be applied to simulate positrons in gases and in models of living tissue. The present model gives an indication of the dissociations induced by higher energy positrons and electrons. We could include a cross-section for dissociative electron attachment, which arises only for secondary electrons at low energies [44, 45], to test how individual events may cause damage, and to establish whether the degree of the damage is associated with the energy deposited to the tissue.

From the provided data, we can conclude that some of the less frequent processes involving a large threshold energy are,

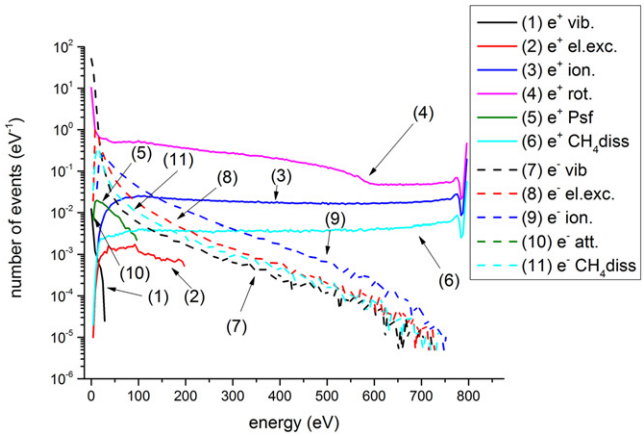


**Figure 5.** Number distribution of collision events against the projectile energy during the thermalization of positrons and secondary electrons. Solid lines represent positron collisions (1—vibrational excitation, 2—electron excitation, 3—ionization, 4—rotational excitation, 5—Ps formation, 6—$CH_4$ dissociation), while the dashed lines represent electron collisions (7—vibrational excitation, 8—electron excitation, 9—ionization, 10—attachment, 11—$CH_4$ dissociation).

in the case of radiation damage, more important than the low energy processes (which is the case for electrons in plasmas) as the initial particles are formed at higher energies. It can also be concluded that the spatial range of these processes goes beyond the range of the initial positrons due to the fact that in some processes newly formed secondary electrons may start with large initial energies. It appears that the critical information required to improve the accuracy of models of positron transport in the human tissue is the partitioning of energy in ionization (we have used the standard data for pure electrons in our simulation [42]).

The model is obviously open to numerous improvements but it is still sufficient to highlight that positron-induced biochemistry may be a field that is open for study, particularly with the new developments in elementary binary collision data, and by using the same tools from the physics of ionized gases, especially the swarm models. Full representation of the organic matter depends on the measurements of a number of cross sections for hydrocarbons, and obtaining a better handle on the representation of the process of solvation of electrons or positrons.

## Acknowledgments

This work was supported by the Grants No. ON171037 and III41011 from the Ministry of Education, Science and Technological Development of the Republic of Serbia and also by the project 155 of the Serbian Academy of Sciences and Arts. SJB and RDW acknowledge financial support of the Australian Research Council through its Centre of Excellence and Discovery Schemes while GG acknowledges financial support from the Spanish Ministerio de Economia y Competitividad (Project FIS2012-31230). SJB also acknowledges the support of the University of Malaya where he holds a Visiting Professor appointment.

## References

[1] Hulett L D Jr, Donohue D L, Xu J, Lewis T A, McLuckey S A and Glish G L 1993 *Chem. Phys. Lett.* **216** 236–40
[2] Passner A, Surko C M, Leventhal M and Mills A P Jr 1989 *Phys. Rev.* A **39** 3706–9
[3] Petrović Z Lj, Banković A, Dujko S, Marjanović S, Malović G, Sullivan J P and Buckman S J 2013 *AIP Conf. Proc.* **1545** 115–31
[4] Banković A, Dujko S, White R D, Marler J P, Buckman S J, Marjanović S, Malović G, Garcia G and Petrović Z Lj 2012 *New J. Phys.* **14** 035003
[5] Bankovic A, Petrovic Z Lj, Robson R E, Marler J P, Dujko S and Malovic G 2009 *Nucl. Instrum. Methods* B **267** 350–3
[6] Šuvakov M, Petrović Z Lj, Marler J P, Buckman S J, Robson R E and Malović G 2008 *New J. Phys.* **10** 053034
[7] Banković A, Marler J P, Šuvakov M, Malović G and Petrović Z Lj 2008 *Nucl. Instrum. Methods* B **266** 462–5
[8] Banković A, Dujko S, White R D, Buckman S J and Petrović Z Lj 2012 *Nucl. Instrum. Methods* B **279** 92–5
[9] Petrović Z Lj, Marjanović S, Dujko S, Banković A, Malović G, Buckman S, Garcia G, White R and Brunger M 2014 *Appl. Radiat. Isot.* **83** 148–54
[10] White R D and Robson R E 2009 *Phys. Rev. Lett.* **102** 230602
[11] Boyle G J, White R D, Robson R E, Dujko S and Petrović Z Lj 2012 *New J. Phys.* **14** 045011
[12] White R D, Dujko S, Robson R E, Petrović Z Lj and McEachran R P 2010 *Plasma Sources Sci. Technol.* **19** 034001
[13] White R D *et al* 2014 *Appl. Radiat. Isot.* **83** 77–85
[14] Makochekanwa C *et al* 2009 *New J. Phys.* **11** 103036
[15] Zecca A, Chiari L, Sarkar A, Lima M A P, Bettega M H F, Nixon K L and Brunger M J 2008 *Phys. Rev.* A **78** 042707
[16] Zecca A, Chiari L, García G, Blanco F, Trainotti E and Brunger M J 2011 *New J. Phys.* **13** 063019
[17] Anderson E K *et al* 2014 *J. Chem. Phys.* **141** 034306
[18] Sánchez-Crespo A, Andreo P and Larsson S A 2004 *Eur. J. Nucl. Med. Mol. Imag.* **31** 44–51
[19] Champion C 2003 *Phys. Med. Biol.* **48** 2147
[20] Reid D D and Wadehra J M 1999 *Chem. Phys. Lett.* **311** 385–9
[21] Champion C and Le Loirec C 2007 *Phys. Med. Biol.* **52** 6605–25
[22] Garcia G, Petrovıc Z L, White R and Buckman S 2011 *IEEE Trans. Plasma Sci.* **39** 2962–3
[23] Fuss M C, Sanz A G, Munoz A, Blanco F, Brunger M J, Buckman S J, Limo-Vieira P and Garcia G 2014 *Appl. Radiat. Isot.* **83** 159–64
[24] Tattersall W, Chiari L, Machacek J R, Anderson E, White R D, Brunger M J, Buckman S J, Garcia G, Blanco F and Sullivan J P 2014 *J. Chem. Phys.* **140** 044320
[25] Baró J, Sempau J, Fernández-Varea J M and Salvat F 1995 *Nucl. Instrum. Methods* B **100** 31
[26] Agostinelli S *et al* 2003 *Nucl. Instrum. Methods* A **506** 250
[27] Haxton D J, McCurdy C W and Rescigno T N 2007 *Phys. Rev.* A **75** 012710
[28] Devins J C, Rzad S J and Schwabe R J 1981 *J. Appl. Phys.* **52** 4531–45
[29] Coe J V, Lee G H, Eaton J G, Arnold S T, Sarkas H W, Bowen K H, Ludewigt C, Haberland H and Worsnop D R 1990 *J. Chem. Phys.* **92** 3980
[30] Huels M A, Boudai B, Cloutier P, Hunting D and Sanche L 2003 *J. Am. Chem. Soc.* **125** 4467–77
[31] Zipf E C 1984 Dissociation of molecules by electron impact *Electron Molecule Interactions and their Applications* vol 1, ed L G Christophorou (London: Academic) p 335
[32] Raspopović Z M, Sakadžić S, Bzenić S and Petrović Z Lj 1999 *IEEE Trans. Plasma Sci.* **27** 1241–8

[33] Petrović Z Lj, Raspopović Z M, Dujko S and Makabe T 2002 *Appl. Surf. Sci.* **192** 1–25
[34] Dujko S, Raspopović Z M and Petrović Z Lj 2005 *J. Phys. D: Appl. Phys.* **38** 2952–66
[35] Ristivojević Z and Petrović Z Lj 2012 *Plasma Sources Sci. Technol.* **21** 035001
[36] White R D, Brennan M J and Ness K F 1997 *J. Phys. D: Appl. Phys.* **30** 810
[37] Petrović Z Lj, Banković A, Dujko S, Marjanović S, Šuvakov M, Malović G, Marler J P, Buckman S J, White R D and Robson R E 2010 *J. Phys.: Conf. Ser.* **199** 012016
[38] Charlton M 2009 *J. Phys.: Conf. Ser.* **162** 012003
[39] Charlton M and Humberston J 2000 *Positron Physics* (New York: Cambridge University Press)
[40] Motohashi K, Soshi H, Ukai M and Tsurubuchi S 1996 *Chem. Phys.* **213** 369–84
[41] Shirai T, Tabata T, Tawara H and Itikawa Y 2002 *At. Data Nucl. Data Tables* **80** 147–204
[42] Opal C B, Peterson W K and Beaty E C 1971 *J. Chem. Phys.* **55** 4100–6
[43] Champion C and Le Loirec C 2006 *Phys. Med. Biol.* **51** 1707–23
[44] Ptasińska S and Sanche L 2007 *Phys. Rev.* E **75** 031915
[45] Gil T J, Resigno T N, McCurdy C W and Lengsfield B H 1994 *Phys. Rev.* A **49** 2642–50